



ELSEVIER

Available online at [www.sciencedirect.com](http://www.sciencedirect.com) ScienceDirect

Proceedings of the Combustion Institute 32 (2009) 2591–2597

---

---

**Proceedings  
of the  
Combustion  
Institute**

---

---

[www.elsevier.com/locate/proci](http://www.elsevier.com/locate/proci)

# Inhibition of atmospheric-pressure $H_2/O_2/N_2$ flames by trimethylphosphate over range of equivalence ratio

O.P. Korobeinichev<sup>a,b,\*</sup>, I.V. Rybitskaya<sup>b</sup>, A.G. Shmakov<sup>a</sup>,  
A.A. Chernov<sup>a</sup>, T.A. Bolshova<sup>a</sup>, V.M. Shvartsberg<sup>a</sup>

<sup>a</sup> *Institute of Chemical Kinetics & Combustion, Novosibirsk 630090, Russia*

<sup>b</sup> *Novosibirsk State University, Novosibirsk 630090, Russia*

---

## Abstract

The effect of equivalence ratio (in the range 1.3–3) and dilution of unburnt gases by nitrogen on speed and the structure of premixed atmospheric-pressure  $H_2/O_2/N_2$  flames without additive and doped with 0.04% of trimethylphosphate ( $(CH_3O)_3PO$ , TMP) was studied experimentally and by modeling. By comparing modeling and experimental results we validated and refined the mechanism for flame inhibition by organophosphorus compounds. Sensitivity analysis of flame speed to reactions of chain branching and chain termination involving phosphorus-containing species revealed some features of the mechanism for inhibition of hydrogen flames of various equivalence ratio and dilution ratio. It was shown that in hydrogen, in contrast to hydrocarbon flames, reactions of radicals with TMP and organophosphorus products of its destruction play important role. The sensitivity analysis revealed the ratio of rates of chain termination reactions involving phosphorus-containing species to chain branching reaction to increase with rising of equivalence ratio and dilution of unburnt gases. Therefore, the inhibition effectiveness of  $H_2/O_2/N_2$  flames expressed as a relative decrease of burning velocity rises in the range of equivalence ratio from 1.1 to 3 (in contrast to hydrocarbon flames) and with dilution of unburnt gases.

© 2009 The Combustion Institute. Published by Elsevier Inc. All rights reserved.

*Keywords:* Organophosphorus compounds; Inhibition; Flame structure; Burning velocity; Premixed flames

---

## 1. Introduction

During last decades a number of researchers showed organophosphorus compounds (OPCs) to be effective inhibitors and fire suppressants of hydrocarbon flames [1–7]. However, addition of OPCs (up to 0.5% by volume) to a low-pressure

hydrogen flames results in a promotion effect, i.e. increase of the flame speed [8]. It was revealed that recombination of atoms and free radicals catalyzed by OPCs combustion products (phosphorus oxides and acids) is an important part of the mechanism for inhibition and promotion of a flame by OPCs. A number of kinetic models for flame inhibition and promotion by OPCs were elaborated. The last and the most justified version of the mechanism, which was developed on the basis of experimental results on speed of TMP-doped  $C_3H_8$ /air flames and quantum-mechanical calculations [9,10] was used for predicting many experimental data including flame suppression

---

\* Corresponding author. Address: Institute of Chemical Kinetics & Combustion, 3, Institutskaya, Novosibirsk 630090, Russia. Fax: +7 383 3307350.

E-mail address: [korobein@kinetics.nsc.ru](mailto:korobein@kinetics.nsc.ru) (O.P. Korobeinichev).

[11], chemical structure of diffusive counterflow [12] and premixed [13] hydrocarbon/air flames doped with OPCs. In spite of a satisfactory prediction of speed and structure of lean and stoichiometric flames, the mechanism predicted concentration profiles of labile species in rich flames with lower accuracy [13]. To explain a sharp decrease of the inhibition effectiveness of hydrocarbon flames at  $\phi$  (equivalence ratio)  $>1.2$ – $1.3$  and a disagreement between modeling and experiment [13], we proposed a formation of inactive P- and C-containing species in rich flames, which are not considered by the model. That is why it was of interest to verify this suggestion and to refine the mechanism by studying a more plain  $H_2/O_2$  flame, which contains no carbon. The goal of the present paper was studying of influence of OPCs additives on speed and structure of atmospheric-pressure  $H_2/O_2/N_2$  flames of various fuel/oxidizer ratios and in validating of earlier developed mechanism by comparing experimental and modeling results.

## 2. Experimental

### 2.1. Measurement of flame speed

The burning velocity was measured using a heat flux method described in [14,15]. The setup design was similar to that in Ref. [16]. Detailed description of experiment is given in [13].

### 2.2. Measurement of flame structure

Premixed laminar  $H_2/O_2/N_2$  flame was stabilized on the flat burner similar to that in Ref. [13]. The profiles of concentration of flame species were measured using molecular beam mass spectrometric setup equipped with quadrupole mass spectrometer MC 7302 with an ion source for soft ionization by electron impact [17]. A quartz probe with orifice of 0.08 mm in diameter and inner angle of 40 deg. was used. The mass peaks corresponding to H, OH, and P-containing species (PCSs) were measured at low-ionization energy (IE) to avoid the contribution of fragmentary ions to the measured peaks. The IE for each of the measured peaks is given in [17].

Systematic errors in measuring mass peak intensities depended strongly on the concentration of the corresponding species and the background and were not higher than 5% (relative) for stable species, 10–15% for H and OH; for PCSs they were 15% for PO,  $PO_2$ , and HOPO, 20% for  $HOPO_2$ , and 25–30% for  $(HO)_3PO$ .

The calibration coefficients for H, O, and OH were determined based on partial equilibrium by three “rapid” reactions:  $H_2 + OH = H_2O + H$ ,  $H_2 + O = H + OH$ , and  $O_2 + H = OH + O$  similarly to [18]. Calibration measurements were made

for the flame with  $\phi = 1.1$  ( $\phi = [H_2]/[H_2]_{st}$ ) and dilution ratio  $D = 0.09$  ( $D = [O_2]/([O_2] + [N_2])$ ), where concentration of  $H_2$ ,  $O_2$ , and  $H_2O$  in post-flame zone is high enough for measurements with appropriate accuracy. The calibration coefficients obtained were used to determine concentration of radicals in the studied flame. We estimated this method of calibration to provide a mean-square error of  $\pm 50\%$ .

### 2.3. Measurement of flame temperature

Temperature profiles in the flames were measured by Pt-Pt+10%Rh  $\Pi$ -shape thermocouples welded from wire 0.02 mm in diameter, covered by a thin layer of  $SiO_2$  to prevent catalytic recombination of radicals on their surfaces. The resulting thermocouple has a diameter of 0.03 mm and a shoulder length of about 3 mm, providing negligible heat losses. The junction of the thermocouple was located at a distance of 0.25 mm from the tip of the probe. Further details of the thermocouple design can be found elsewhere [19].

## 3. Modeling approach

The simulation of flame structure and burning velocity calculations were performed with the use of PREMIX and CHEMKIN codes. Experimentally measured temperature profiles were used as input data for flame structure simulations.

The flame structure was simulated using a mechanism [10], which included 210 elementary stages and 41 species.

## 4. Results and discussion

### 4.1. Effect of the equivalence ratio and the degree of dilution with an inert on the speed of a $H_2/O_2/N_2$ flame doped with TMP

Figure 1 presents the measured speeds of  $H_2/O_2/N_2$  flames versus  $\phi$  in the range from 0.32 to 2.8 with the dilution ratio  $D$  in the range from 0.209 to 0.077. The same figure shows data [20] obtained using a counterflow burner for a combustible mixture at room temperature and converted to the conditions of our experiments ( $t_0 = 35^\circ C$ ). Good agreement between our and literature data indicates the correctness of our measurements. The flame speeds predicted by the model are slightly lower than the experimental data.

The addition of 0.04% TMP (by volume) to the flames leads to a significant decrease in their speed. Figure 2 gives the measured flame speeds (symbols) and those calculated (dashed curves) using the model of [10] versus  $\phi$  for a flame doped with TMP. It is evident from Fig. 2 that the experimental and calculated results differ by a factor of

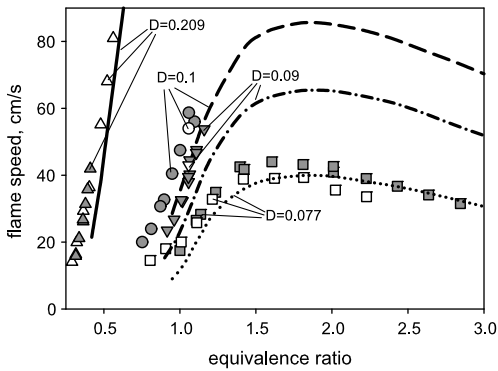


Fig. 1. Speed of  $H_2/O_2/N_2$  flames with different dilution ratios ( $D$ ) versus equivalence ratio; symbols – experiment (gray symbols – our data, open symbols [20]), lines – modeling.

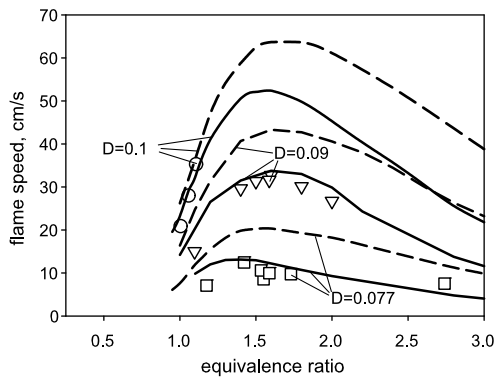


Fig. 2. Speed of  $H_2/O_2/N_2$  flames doped with 0.04% TMP with different  $D$  versus equivalence ratio; symbols – experiment, dashed lines – modeling using mechanism [10], solid lines – modeling using the updated mechanism.

1.3–2. This difference, however, is not due to systematic measurement errors. The observed disagreements between the measured and calculated speeds are different for flames with and without TMP additives: for undoped flames, the flame speed predicted by the model is slightly underestimated, and for flames with the additive, it is overestimated.

An analysis of the speed sensitivity of a  $H_2/O_2/N_2$  flame doped with TMP with respect to the rate constants of the reactions involving P-containing

species shows that, in contrast to hydrocarbon–air flames, the  $H_2/O_2/N_2$  flame speed is the most significantly sensitive to the primary stages involving TMP and its primary destruction products, which proceed in the low-temperature flame zone. These reactions are given in Table 1. It should be noted that in methane–air and propane–air flames, the flame speed was most significantly affected by the atom and radical recombination reactions involving phosphorus oxyacids, which proceed in the high-temperature flame zone [17]. Because the rate constants of the stages presented in Table 1 have previously been estimated only approximately [21], we changed the preexponential factors of their rate constants as is shown in Table 1 in order to obtain agreement between the calculated and measured speeds of TMP-doped flames.

The results of flame speed calculations using the changed reaction rate constants are given in Fig. 2. It is evident that the changed mechanism provides an adequate description of the experimental data on the effect of TMP additives on the  $H_2/O_2/N_2$  flame speed. We note that the sensitivity coefficients for the same reactions in  $CH_4$ /air flames doped with TMP are negligibly small. For example, for a  $CH_4$ /air flame ( $\phi = 1.1$ , 0.06% TMP), the flame speeds calculated for the original mechanism and the mechanism with the changed rate constants of the three reactions given above differ by only 0.2%. Thus, the changed mechanism describes the propagation speed of both hydrocarbon–oxygen and hydrogen–oxygen flames doped with TMP. The calculations showed that the change in the rate constants of the reactions did not lead to appreciable changes in the flame structure for  $\phi = 1.6$ , including the concentration profiles of the final products of TMP conversion – PO,  $PO_2$ , HOPO, and  $HOPO_2$ .

The changed rate constants of the three reaction were used to calculate the dependence of the inhibition effectiveness  $F$  ( $F = (U_0 - U)/U_0$ , where  $U_0$  and  $U$  are the speeds of the undoped flames and flames doped with 0.04% TMP, respectively) on  $\phi$ . The calculated dependences are presented in Fig. 3. It can be seen that  $F$  increases as  $\phi$  increases from 1 to 3 and as  $D$  decreases from 0.209 to 0.077. Modeling data with updated mechanism for  $D = 0.077$  are in a good agreement with experiment.

It is important to note that the dependence of  $F$  on  $\phi$  for  $H_2/O_2/N_2$  differs from that for

Table 1  
Three important reactions and pre-exponential factors of their rate constants before and after modification

Reaction	$A$ [ $10^{\text{st}}$ ]	$A_{\text{modified}}^a$
$(CH_3O)_3PO + H = (CH_3O)_2PO(OCH_2) + H_2$	$2.2 \times 10^9$	$4.4 \times 10^9$
$(CH_3O)_2PO(OCH_2) + O = OP(OCH_3)_2O + CH_2O$	$5.0 \times 10^{13}$	$1.0 \times 10^{13}$
$(CH_3O)_2PO(OCH_2) = OP(OCH_3)_2 + CH_2O$	$2.0 \times 10^{13}$	$2.0 \times 10^{12}$

<sup>a</sup> Units are  $\text{cm}^3$ , mol, s.

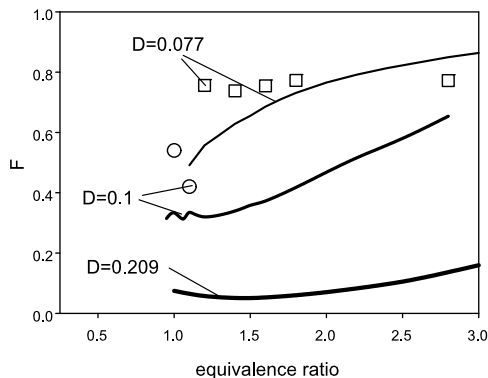


Fig. 3. Inhibition effectiveness  $F$  for  $H_2/O_2/N_2$  flames doped with 0.04% TMP with different dilution ratios ( $D$ ) versus equivalence ratio; symbols – experiment, lines – modeling using the updated mechanism.

hydrocarbon flames [13,22]. In hydrocarbon flames doped with 0.06% TMP, the inhibition effectiveness  $F$  increases slightly as  $\phi$  increases from 0.7 to 1.2–1.3, and a further increase in  $\phi$  from 1.3 to 1.5 leads to an abrupt decrease in  $F$  by a factor of 1.5 to 2 [13].

The addition of TMP to flames reduces the maximum concentration of H atoms in the chemical reaction zone of a flame. Figure 4 shows the relative reduction in the maximum concentration of H atoms  $\Delta[H]_{\max}$  ( $\Delta[H]_{\max}=1 - [H]_{\max}^d/[H]_{\max}^0$ ) and OH radicals  $\Delta[OH]_{\max}$  ( $\Delta[OH]_{\max}=1 - [OH]_{\max}^d/[OH]_{\max}^0$ ) due to the addition of TMP versus  $\phi$ , obtained from structure simulations for freely-propagating flames without additives and with 0.04% TMP added. Where  $[H]_{\max}$  and  $[OH]_{\max}$  – maximal concentrations of H and OH in the flame zone, superscripts “d” and “0” are related to doped and clear flames, respectively. It is evident from Figs. 3 and 4, that there is a cor-

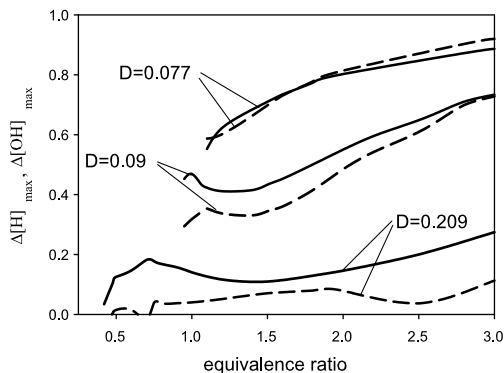


Fig. 4. Relative decrease of H (solid lines) and OH (dashed lines) maximal concentration in flames doped with 0.04% TMP with different  $D$  versus equivalence ratio; modeling data using the updated mechanism.

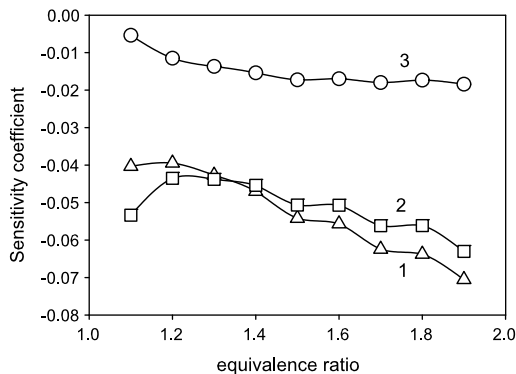
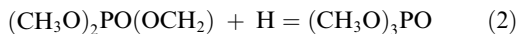
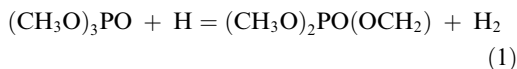


Fig. 5. Sensitivity coefficients of speed of  $H_2/O_2/N_2$  flames ( $\phi = 1.6$ ,  $D = 0.077$ , 0.09, and 0.209) doped with 0.04% TMP to rate constants of reactions (1)–(3) involving P-containing species; modeling is based on mechanism [10].

relation between the dependences of  $F$  and  $\Delta[H]_{\max}$  and  $\Delta[OH]_{\max}$  on  $\phi$  and  $D$ .

An analysis of the flame speed sensitivity coefficients with respect to the reaction rate constants for a flame with  $D = 0.09$  shows (Fig. 5) that an increase in  $\phi$  from 1.1 to 1.9 primarily enhances the role of the reactions of hydrogen atoms with TMP and its primary destruction product:



and the reactions with the HOPO species:



These reactions are involved in the catalytic recombination cycles of H atoms with the formation of  $H_2$ . It is these reactions that are responsible for the rise in the inhibition effectiveness with increasing of  $\phi$ . Generally, speaking about catalytic cycles, responsible for scavenging of radicals in OPC-doped flames, we usually mean reactions involving phosphorus oxides and acids because reactions of organophosphorus compounds in most cases play minor role in inhibition processes. But in these specific flames reactions of OPCs with active species are of importance.

An analysis of the speed sensitivity coefficients of TMP-doped  $H_2/O_2/N_2$  flames with respect to the rate constants of the main hydrogen combustion reactions and the reactions involving P-containing species revealed the main stages responsible for an increase in  $F$  with decreasing  $D$ . From the data given in Fig. 6 for the main hydrogen combustion reactions, it is evident that a decrease in  $D$  leads primarily to a growth in the role of the  $H + O_2 = O + OH$  branching reaction. In flames with  $\phi = 1.6$ , the flame speed sensitivity coefficient with respect to the rate constant

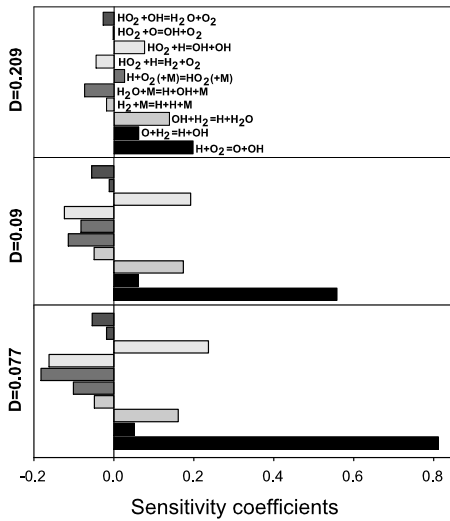


Fig. 6. Sensitivity coefficients of speed of  $\text{H}_2/\text{O}_2/\text{N}_2$  flame ( $\phi = 1.6$ ,  $D = 0.077$ ,  $0.09$ ,  $0.209$ ) doped with 0.04% TMP to rate constants of 10 key reactions of hydrogen combustion.

of this reaction increased by a factor of 4 as  $D$  decreased from 0.209 to 0.077. In addition, the sensitivity coefficient for this reaction is much larger than that of the remaining reactions. Furthermore, dilution with  $\text{N}_2$  changes the role of the  $\text{H} + \text{O}_2(+\text{M}) = \text{HO}_2(+\text{M})$  recombination reaction, for which the sensitivity coefficient is negative for flames with dilution coefficients  $D = 0.077$  and  $D = 0.09$  and is positive for  $D = 0.209$ .

However, an analysis of the flame speed sensitivity to the rate constants of chain termination reactions – radical recombination upon interaction with TMP and its destruction products (Fig. 7) – show that decreasing  $D$  increases the sensitivity to these reactions much more strongly than the sensitivity to the branching reaction constant rate. For example, as  $D$  decreases from 0.209 to 0.077, the sensitivity coefficient with respect to the rate constants of reactions (1) and (2) increases by a factor of 8 and 20 times, respectively. This is much greater than the increase in the flame speed sensitivity coefficient with respect to the branching reaction. An analysis of the simulation results shows that, a decrease in  $D$  from 0.209 to 0.077 also results in a factor of 2–5 increase in the ratio of the maximum rate of recombination of H atoms by reactions (1) and (2) to the maximum rate of the branching reaction. It is this factor that is responsible for the increase in the inhibition effectiveness  $F$  with decreasing  $D$ , and, possibly, for the increase in  $F$  with increasing of  $\phi$ . Thus, the ratio of the chain termination rate to the chain branching rate is an important parameter that determines the hydrogen–oxygen flame speed.

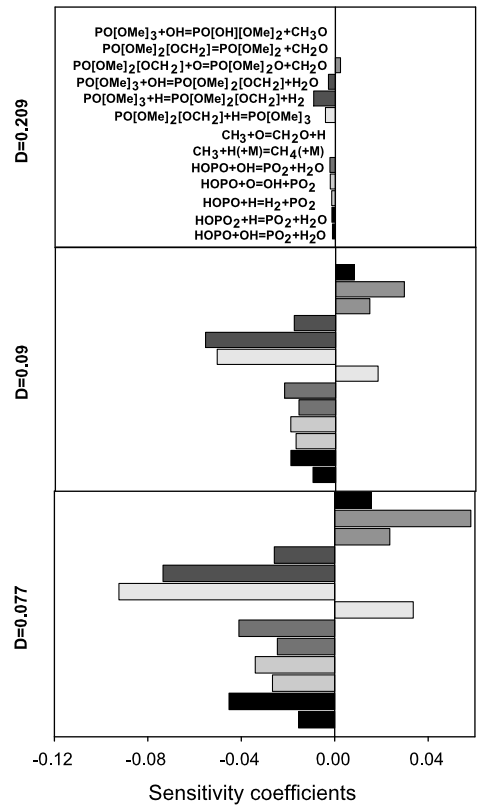


Fig. 7. Sensitivity coefficients of speed of  $\text{H}_2/\text{O}_2/\text{N}_2$  flame ( $\phi = 1.6$ ,  $D = 0.077$ ,  $0.09$ ,  $0.209$ ) doped with 0.04% TMP to rate constants of 13 key reactions of the inhibition mechanism [10] involving P-containing species.

#### 4.2. Structure of rich flames $\text{H}_2/\text{O}_2/\text{N}_2$ flames doped with TMP

For a rich  $\text{H}_2/\text{O}_2/\text{N}_2$  flame doped with 0.04% TMP with an equivalence ratio  $\phi = 1.6$  and  $D = 0.09$ , temperature and concentration profiles of stable species ( $\text{O}_2$ ,  $\text{H}_2\text{O}$ ), radicals (H and OH), and P-containing species PO, HOPO,  $\text{PO}_2$ , and  $\text{HOPO}_2$  were measured and simulated. The simulation was performed with the use of mechanism [10], in which the rate constants of three reactions were changed. The measured and simulated concentration profiles of the stable species ( $\text{O}_2$ ,  $\text{H}_2\text{O}$ , TMP) were compared and found to be in satisfactory agreement (within experimental errors). Figure 8 gives the measured and simulated concentration profiles for H and OH. The change in the rate constants of the reactions given in Table 1 had no significant effect on the simulated concentration profiles of H atoms and OH radicals.

In the flame at a distance of 2–15 mm from the burner surface, the main P-containing species are

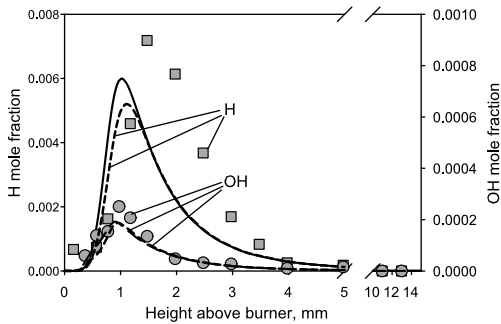


Fig. 8. Profiles of concentration of H and OH in  $H_2/O_2/N_2$  flame ( $\phi = 1.6$ ,  $D = 0.09$ ) doped with 0.04% TMP; symbols – experiment, solid lines – modeling using mechanism [10], dashed lines – modeling using the updated mechanism.

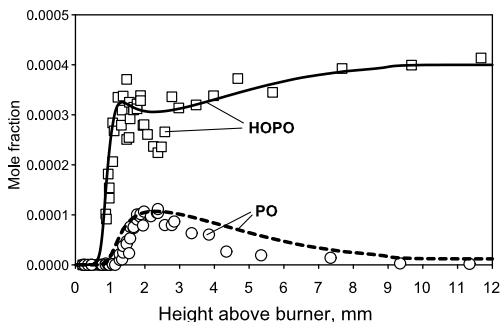


Fig. 9. Profiles of concentration of PO and HOPO in  $H_2/O_2/N_2$  flame ( $\phi = 1.6$ ,  $D = 0.09$ ) doped with 0.04% TMP; symbols – experiment, lines – modeling using the updated mechanism.

PO and HOPO. Their concentration profiles in the flame are presented in Fig. 9. The PO concentration in the combustion zone increases and reaches the maximum at a distance of 2 mm from the burner surface, after which it decreases to almost zero at a distance of 6–8 mm. The results of the study show that the updated mechanism provides a good description of the experimental flame structure data.

## 5. Summary

This study performed revealed a number of features of the mechanism for inhibition of diluted  $H_2/O_2/N_2$  flames at atmospheric-pressure. It was shown that inhibition effectiveness, expressed as a relative decrease of flame speed or maximal H and OH concentration with addition of the inhibitor, in contrast to hydrocarbon flames, increases with rising of  $\phi$  and decreasing of  $D$ . The sensitivity analysis revealed that it occurs due to a rise of ratio of rate of chain termination in reactions

involving the inhibitor to rate of chain branching. This in its turn occurs because of a decrease of flame temperature with increasing of  $\phi$  and dilution. It is noteworthy that the change of composition of phosphorus species with  $\phi$  also contributes to a rise of the inhibition effectiveness [10]. The reducing of flame temperature appreciably influences on rate of chain branching and only slightly on chain termination through reactions involving the inhibitor. It happens due to low-activation energies of key reactions, responsible for inhibition, and relatively high activation energy of chain branching reaction.

The earlier developed mechanism for flame inhibition by OPCs was shown to predict unsatisfactorily the speed of strongly diluted  $H_2/O_2/N_2$  flames doped with OPCs. The sensitivity analysis demonstrated the reaction of radicals with TMP and some products of its destruction to play major role in these flames. The modification of rate constants of three important reactions (within accuracy of their determination) allowed obtaining a satisfactory agreement between simulated and measured speed of the flames.

## Acknowledgments

This work was supported by INTAS under Grant 03-51-4724 and by Russian Foundation of Basic Research under grants # 05-03-34815-MF\_a and 07-03-01000-a. The authors thank Dr. Alexander Konnov and Professor A. Baratov for fruitful discussion and help.

## References

- [1] J.W. Hastie, D.W. Bonnell, Molecular of Inhibited Combustion Systems, National Bureau of Standards, NBSIR 80-2169, 1980.
- [2] A.J. Twarowski, *Combust. Flame* 94 (1993) 91–107.
- [3] J.H. Werner, T.A. Cool, *Combust. Flame* 117 (1999) 78–98.
- [4] P.A. Glaude, C. Melius, W.J. Pitz, C.K. Westbrook, *Proc. Combust. Inst.* 29 (2002) 2469–2476.
- [5] R.T. Wainner, K.L. McNesby, A.W. Daniel, A.W. Miziolek, V.I. Babushok, Halon Options Technical Working Conference (HOTWC), Albuquerque, NM, 2000, pp. 141–153.
- [6] A.G. Shmakov, O.P. Korobeinichev, V.M. Shvartsberg, D.A. Knyazkov, T.A. Bolshova, I.V. Rybitskaya, *Proc. Combust. Inst.* 30 (2005) 2345–2352.
- [7] J.D. Mather, R.E. Tapscott, J.M. Shreeve, R.P. Singh, in: R.G. Gann, S.R. Burgess, K.C. Whisner, P.A. Reneker (Eds.), CD-ROM, NIST SP 948-3, National Institute of Standards and Technology, Gaithersburg, MD, 2005.
- [8] O.P. Korobeinichev, T.A. Bolshova, V.M. Shvartsberg, A.A. Chernov, *Combust. Flame* 125 (2001) 744–751.

- [9] O.P. Korobeinichev, V.M. Shvartsberg, A.G. Shmakov, *Proc. Combust. Inst.* 30 (2005) 2353–2360.
- [10] T.M. Jayaweera, C.F. Melius, W.J. Pitz, *Combust. Flame* 140 (2005) 103–115.
- [11] A.G. Shmakov, O.P. Korobeinichev, V.M. Shvartsberg, *Combust. Explos. Shock Waves* 42 (6) (2006) 678–687.
- [12] D.A. Knyazkov, A.G. Shmakov, O.P. Korobeinichev, *Combust. Flame* 151 (2007) 37–45.
- [13] O.P. Korobeinichev, V.M. Shvartsberg, A.G. Shmakov, D.A. Knyazkov, I.V. Rybitskaya, *Proc. Combust. Inst.* 31 (2007) 2741–2748.
- [14] L.P.H. de Goey, A. Van Maaren, R.M. Quax, *Combust. Sci. Technol.* 92 (1993) 201–207.
- [15] A. Van Maaren, D.S. Thung, L.P.H. de Goey, *Combust. Sci. Technol.* 96 (1994) 327–344.
- [16] I.V. Dyakov, A.A. Konnov, J. de Ruyck, K.J. Bosschaert, E.C.M. Brock, L.P.H. de Goey, *Combust. Sci. Technol.* 172 (2001) 81–96.
- [17] O.P. Korobeinichev, V.M. Shvartsberg, A.A. Chernov, *Combust. Flame* 118 (4) (1999) 727–732.
- [18] O.P. Korobeinichev, V.M. Shvartsberg, S.B. Il'in, A.A. Chernov, T.A. Bolshova, *Combust. Explos. Shock Waves* 35 (3) (1999) 239–244.
- [19] O.P. Korobeinichev, S.B. Ilyin, V.V. Mokrushin, A.G. Shmakov, *Combust. Sci. Technol.* 116 (1996) 51–61.
- [20] F.N. Egolfopoulos, C.K. Law, *Proc. Combust. Inst.* 23 (1990) 333–340.
- [21] P.A. Glaude, H.J. Curran, W.J. Pitz, C.K. Westbrook, *Proc. Combust. Inst.* 28 (2000) 1749–1756.
- [22] I.V. Rybitskaya, A.G. Shmakov, O.P. Korobeinichev, *Combust. Explos. Shock Waves* 43 (3) (2007) 253–257.